

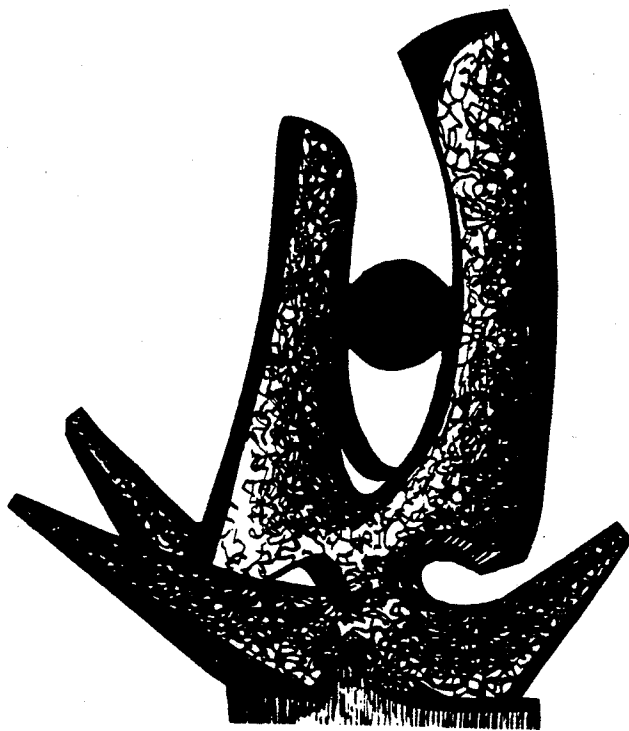
MICHIGAN STATE UNIVERSITY

CYCLOTRON LABORATORY

A REVIEW OF STUDIES FOR THE VARIABLE FREQUENCY  
SUPERCONDUCTING ECR ION SOURCE PROJECT AT MSU

T.A. ANTAYA

INVITED PAPER PRESENTED AT INTERNATIONAL CONFERENCE ON PHYSICS OF  
MULTIPLE CHARGED IONS, GRENOBLE, FRANCE -- SEPTEMBER 1988



NOVEMBER 1988

**Abstract-** The SC-ECR ion source is now under construction at MSU. In this paper, studies undertaken in conjunction with this ion source project will be reviewed. The magnet design studies were expanded to include a high-mirror-ratio axial profile, and we have completed a review of the impact of this possible design change on the solenoid coil structure. Upcoming tests of the prototype solenoid coil structure will be described. Hexapole coils have been wound and successfully tested, and we will summarize those results. In order to establish a basis for selecting the axial field profile, the RT-ECR was modified to operate on a two mirror profile with a high mirror ratio on the first stage side, and the results of this study will be presented. A key component of that test was a simple, single transmitter feed for both stages that is under consideration for the high frequency injection structure for the SC-ECR. Several new ECR beam formation studies have been initiated. ERAY calculations suggest that the angular tilt of the puller electrode nose has an important effect on the extracted emittance. In another study, we properly measured the voltage dependence of the RT-ECR total extracted current, and can identify two regimes of operation. Recent emittance measurements on the RT-ECR will be discussed. We have also measured the energy spread of argon ions through  $10^+$ , and new aspects of these measurements will be reported, including: observation of higher energy low charge ions, a preliminary explanation of the gas mixing effect in ECR sources as an ion cooling process, and observation of an ion energy dependence on rf power.

## 1- INTRODUCTION

The SC-ECR, is a two stage superconducting ECRIS with a hexapole stabilized triple axial mirror confinement structure /1/. A major goal of this project is to build and operate an ECRIS with a potential first harmonic resonance heating range of 6-35 GHz, and to then push up the frequency from the known CW operating range of 6-14 GHz, to 28-35 GHz, as higher frequency power sources become available at MSU. The initial operation, at 6.4 GHz or 14 GHz, will be considerably enhanced by having a confinement structure with such a wide dynamic range. As initially e, the SC-ECR is an extrapolation of the 2 Minimum B mode of operation of the RT-ECR at MSU /2/. The SC-ECR design is shown in Fig. 1.

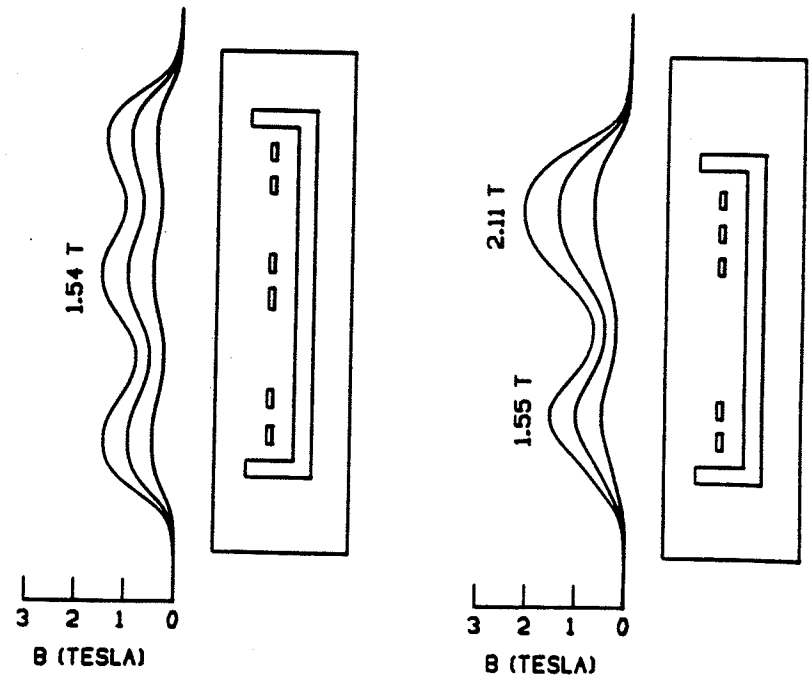


Fig. 2. Two axial magnetic field profiles are under consideration. The 3 mirror profile on the left produces a field equivalent to that of the RT-ECR. The profile on the right is similar to that of the Grenoble 2B Caprice ECRIS [7,8]. Both profiles are shown for 1/3, 2/3 and full coil excitation.

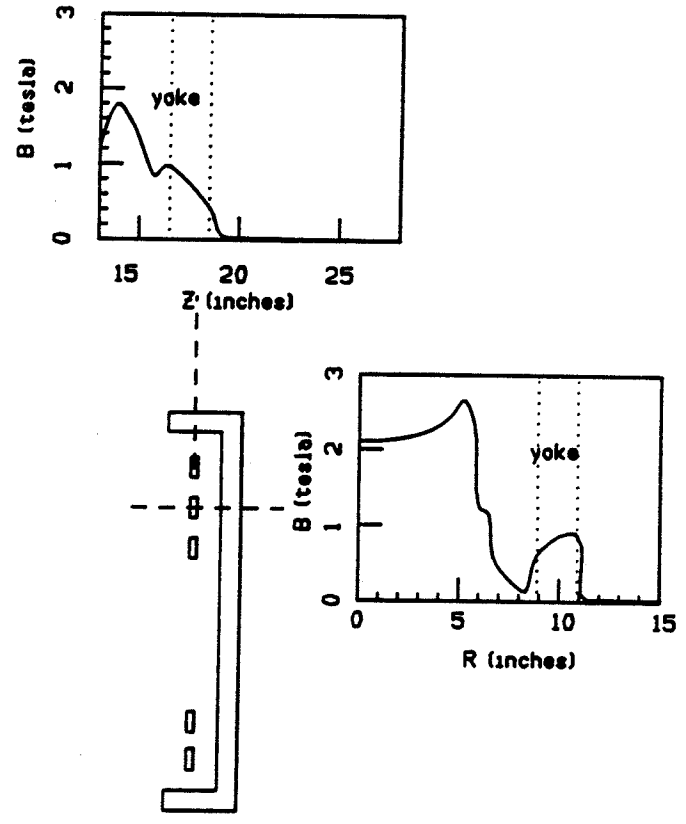


Fig. 3. The magnetic field in the iron return yoke is shown for two locations adjacent to solenoid coils.

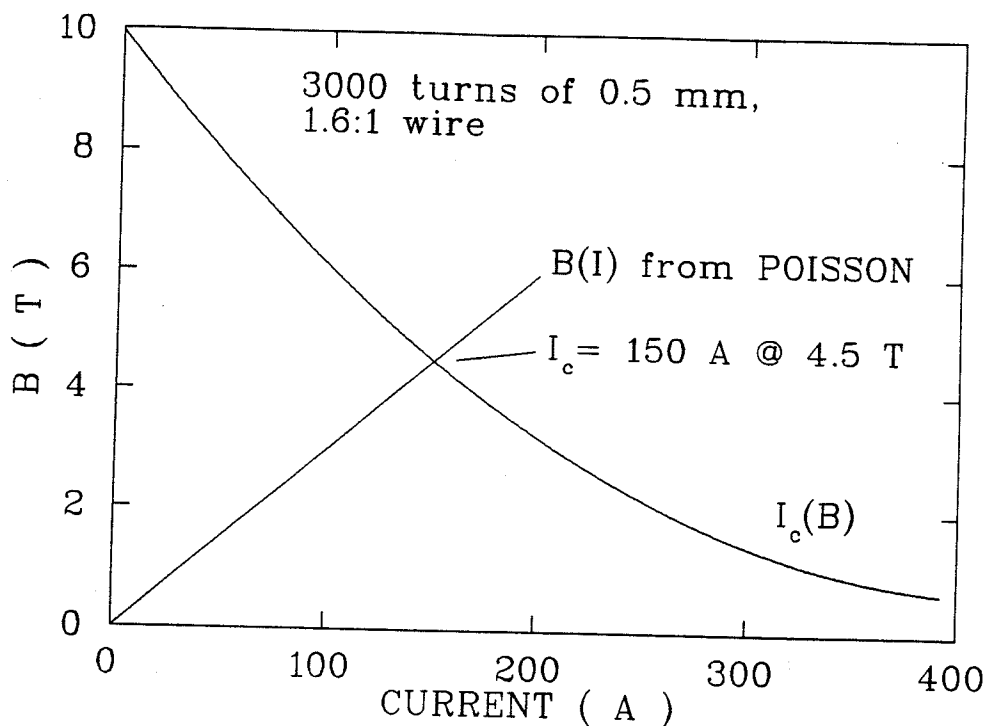


Fig. 6. The operating diagram for single prototype solenoid coils. The  $I_c(B)$  curve is taken from conductor properties; the  $B(I)$  curve follows the peak field in the coil itself. The intersection is the critical current quench point.

A similar analysis has already been completed for the hexapole coil design. For this magnet, the required design excitation is shown in Fig. 7. To minimize the required coil excitation, the cryostat inner bore is thin (not shown). The principle operating constraints are the peak field and stored energy. The peak field in the hexapole, due to the hexapole itself, is 3.25 T and occurs at the ends, as shown in Fig. 8. The addition of the end solenoid coil can add to or subtract from this peak field, so both cases must be considered, as shown in Fig. 9. There is also a 60 degree alternation of the sign of the net force as well, and as a consequence, hexapole coils must be well constrained at the ends. The six

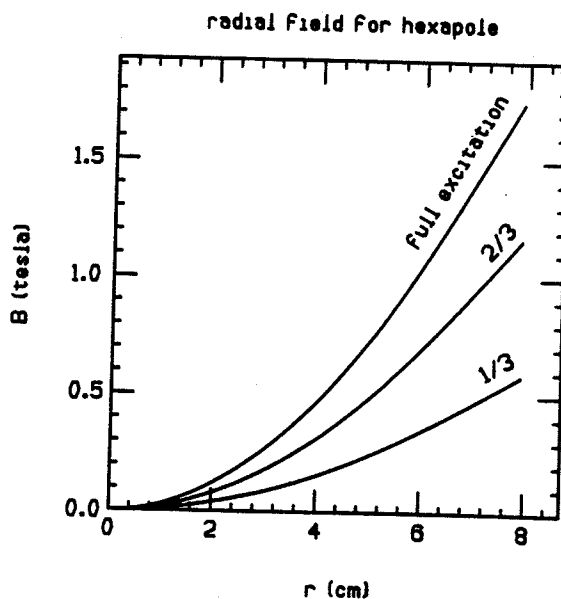


Fig. 7. The required hexapole magnet radial field is shown, for 1/3, 2/3 and full excitation of the coils. The hexapole spans the length of the ion source inside the solenoid coil radius.

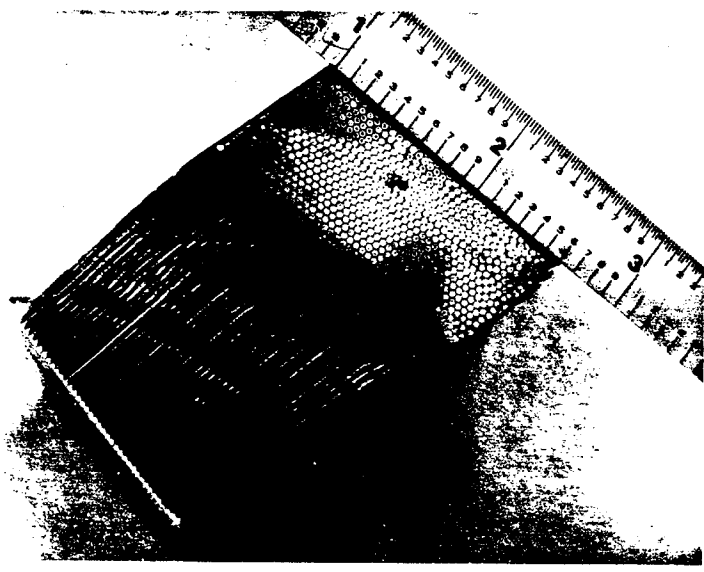


Fig. 10. A section through the end of a test hexapole coil shows a well ordered winding, achieved by using a constant length form shape.

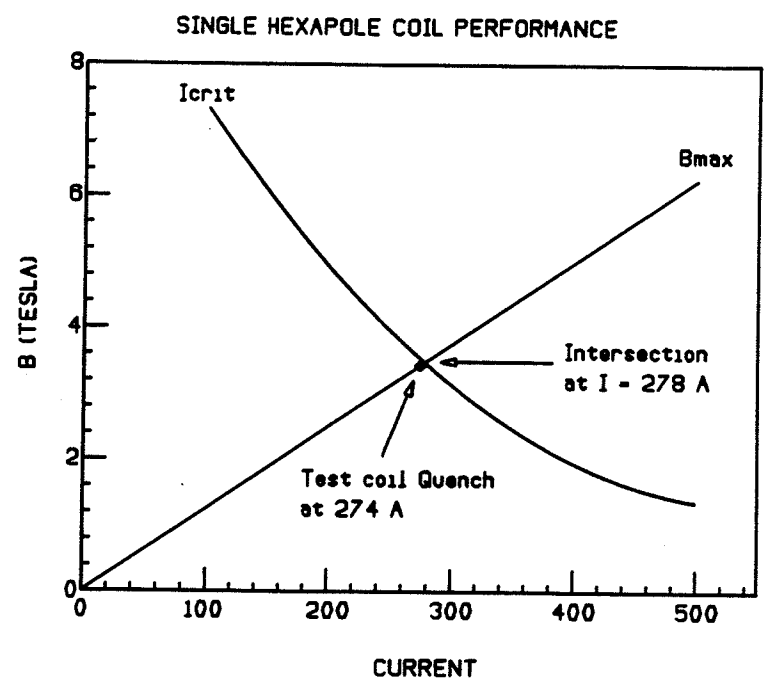


Fig. 11. The operating diagram for single hexapole coils is shown. The intersection of the coil peak field curve ( $B_{max}$ ) with the conductor critical current ( $I_{crit}$ ) occurs at 278 A. Test coils quenched near this predicted limit without training in tests at Fermilab.

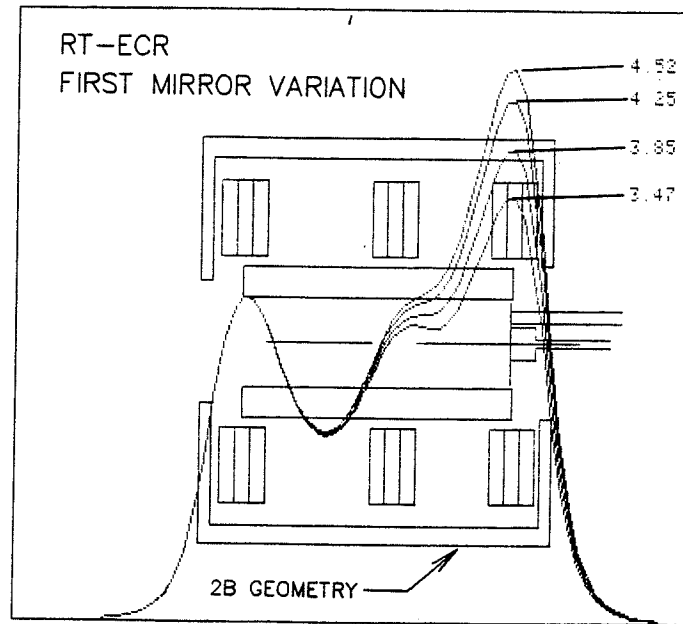


Fig. 13. The relationship between the axial field profile and the 2B geometry is shown. In the 2B mode, the first mirror is obtained by operating the first three coils near maximum excitation, while the middle group is used to adjust the mirror ratio. The main stage resonance zone is nearly independent of the adjustment of the strength of the first mirror.

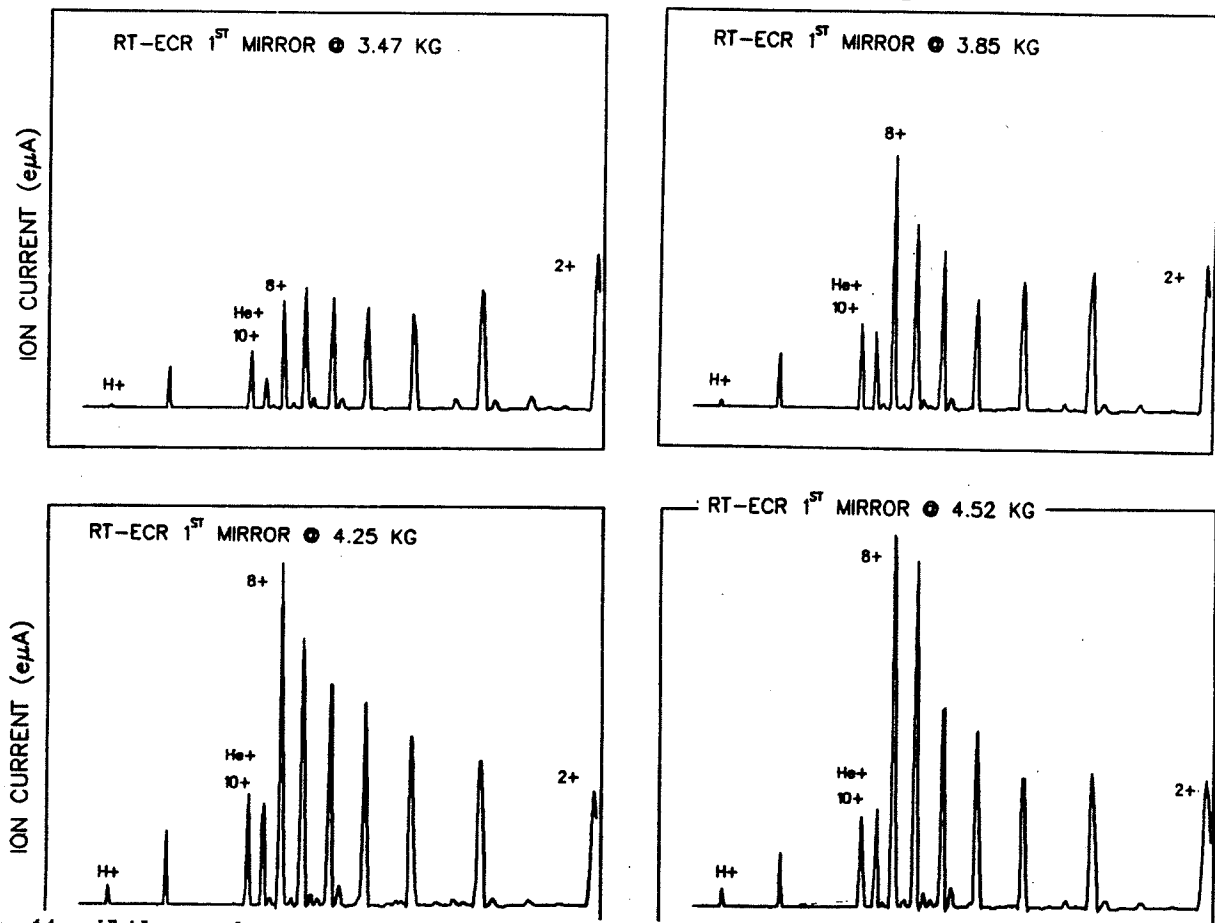


Fig. 14. While no sharp resonance-like effect was observed in raising the first mirror to the 2B level, a more general mirror dependent of the source output was observed. The argon charge state distribution is seen to shift towards higher currents of highly charged ions as the first mirror in the steps shown in Fig. 13. All four plots are plotted at the same full scale current of 40 microamps. The only source parameter varied was the first mirror strength.

Experimentally, we found this to be the case. The sum of the currents on the puller electrode, 4-jaw collimator (not shown) and adjustable slit before this faraday cup were never more than a few percent of the current measured on the faraday cup. In particular, the current on the 4-jaw collimator was consistent with the level of helium 2+ ions in the plasma, over-focused by the lens setting for 1+.

The results of this measurement are summarized in Fig. 16. The three experimental curves correspond to helium feed pressures to give total extracted currents of 0.5, 1.0 and 2.0 emA at a source bias voltage of 12.5 kV (the feed rate was raised to raise the output). No other source parameters were changed. The line marked theory corresponds to a Pierce gun calculation for an aperture of 8mm and an extraction gap of 3.2 cm. The results show two regimes of significance. At low voltage, the total extracted current is found to be space-charge limited emission. At high voltage, the total extracted current becomes constant. The transition voltage, where the source output shifts from space-charge limited to constant current operation, increases as the plasma density increases. Hence the bias voltage must increase as source density is increased to extract all the 'available' current in high density ECRIS.

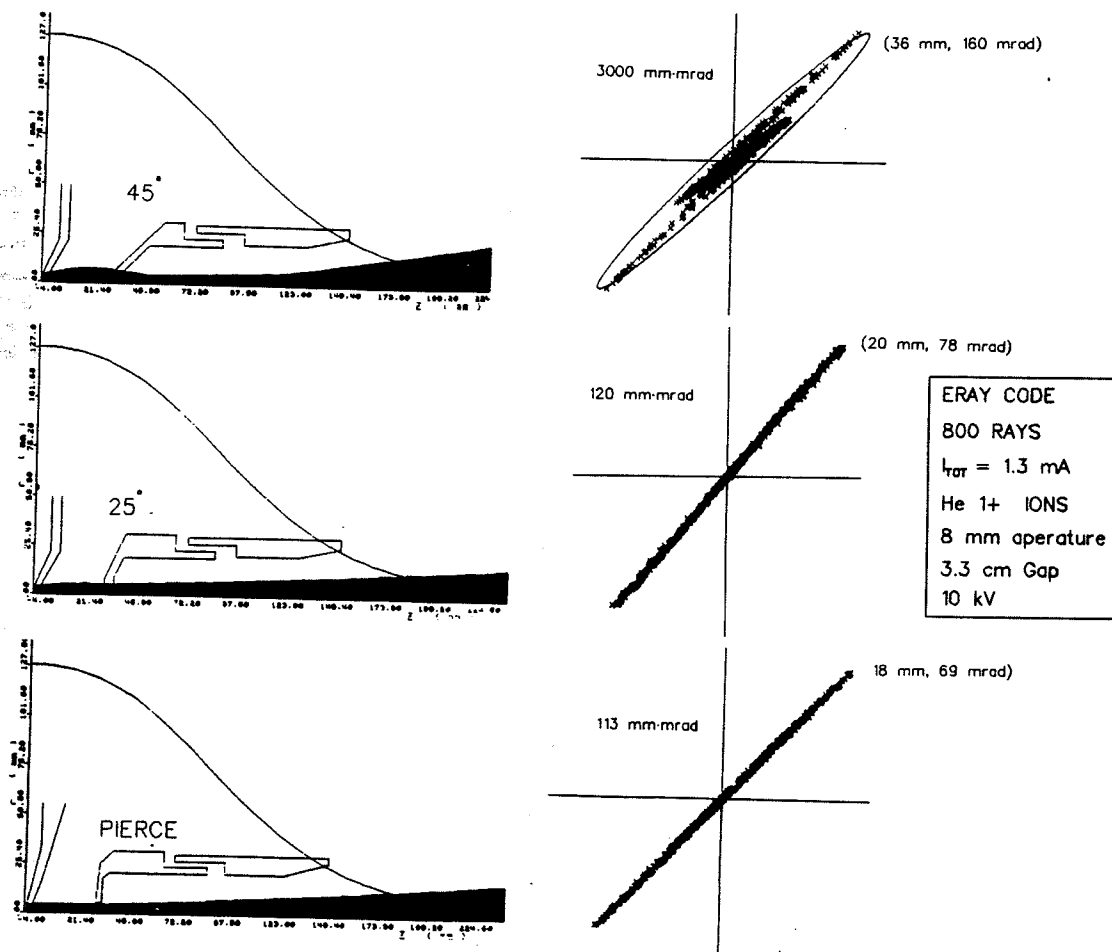


Fig. 15. ERAY /9/ calculations are shown for 1.3 mA of helium 1+ ions extracted at 10 kV, for different puller electrode edge angles. The calculated emittance after extract is shown for each case. The 45 degree puller angle geometry is the present extraction geometry of the NSCL RT-ECR ion source, and was adapted from the LBL Design /10/. In all 3 cases the source extraction aperture has the classical 67.5 degree angle.

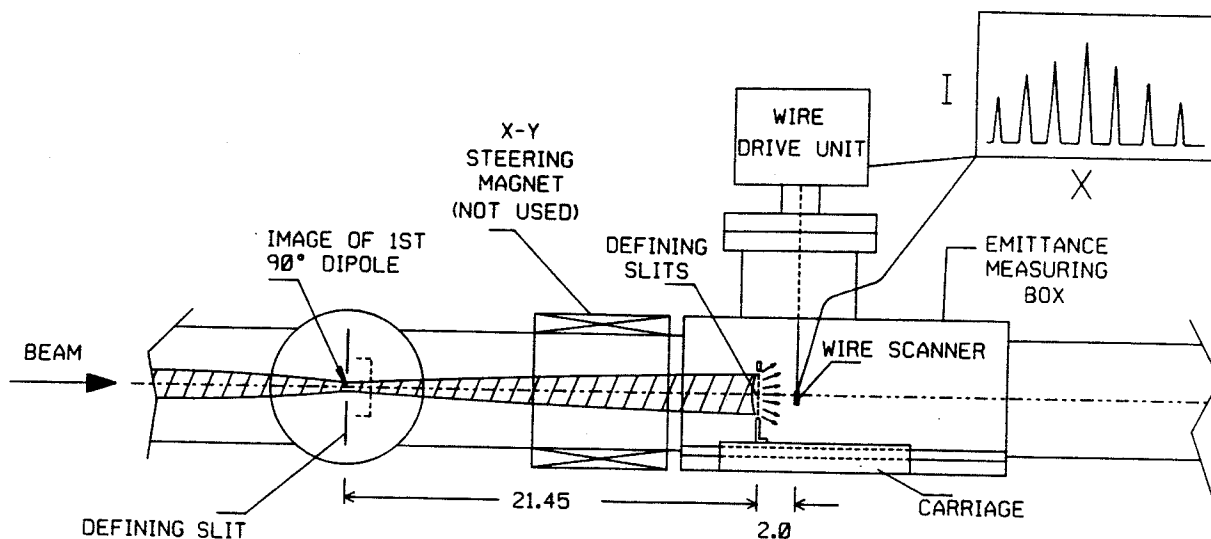


Fig. 17. A vertical defining slit and wire scanner located in a field free region after the image of the first  $90^\circ$  degree dipole are used to measure the vertical emittance of the RT-ECR.

### He<sup>+</sup> Wire Scans After Analysis Dipole Image Slit

Obj. x Img. Slits: 5 mm x 5 mm, 10x10, 20x20, 30x30

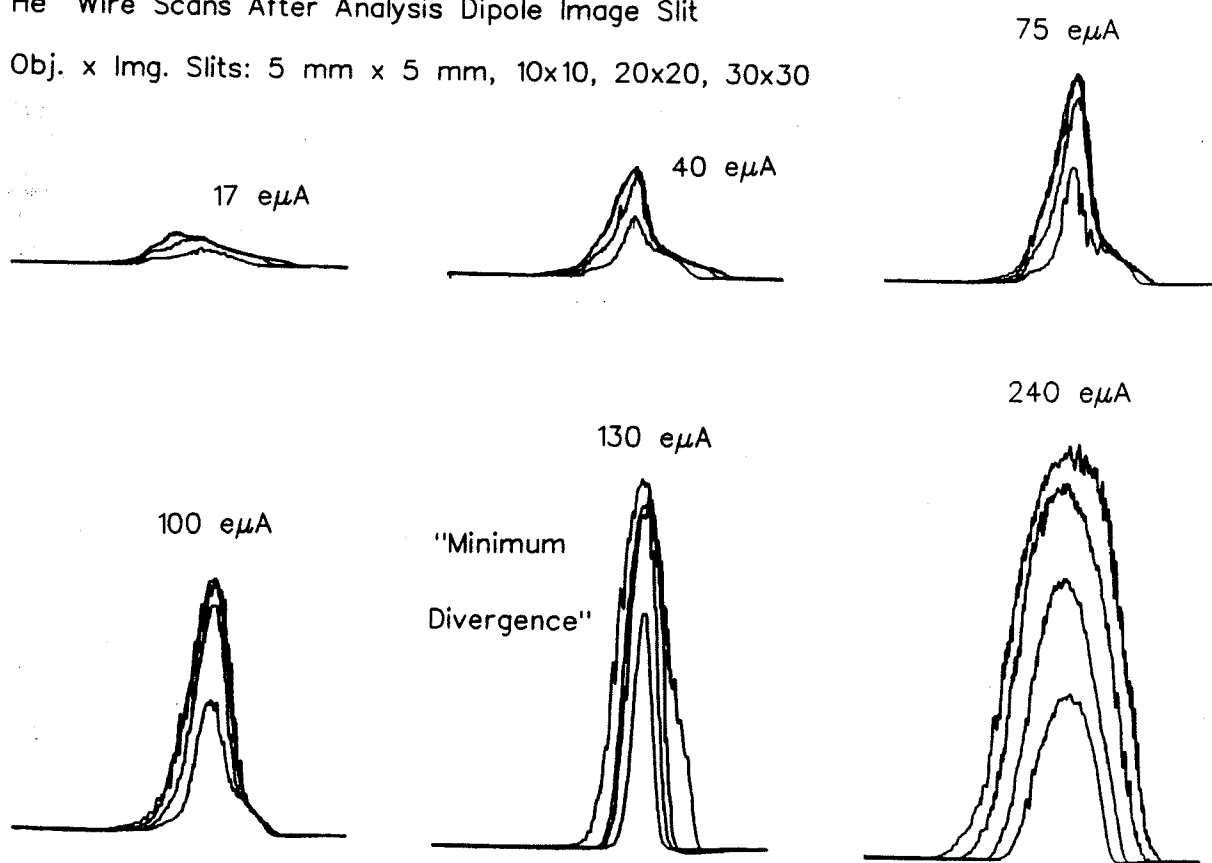


Fig. 18. With the emittance defining slit removed, the divergence profile of helium +1 beams have been scanned as a function of analysis slit setting and intensity. At high intensity, a high measured divergence would be expected on the basis of the high space charge forces acting on the beam, and this is seen in the 240 microamp scans. However, helium beams exhibit high divergence at low intensity as well, and there seems to be an intermediate intensity at which the high divergence component is cancelled.



### ORIGIN OF THE GAS MIXING EFFECT

We have just made energy spread measurements that may explain the gas mixing effect in ECR sources. There has not been adequate time to make a complete analysis, we report here our preliminary results with a preliminary analysis.

At the last ECR meeting, R. Geller presented a plausible explanation for the observed gas mixing effect in ECRIS /14/. On the basis of this model, however, hydrogen should universally be the best mixing gas, for a mostly hydrogen plasma would always have an average charge somewhere between 0.5 and 1.0. We almost never find hydrogen to be the best mixing gas. Instead, we see gas mixing effects like that for RT-ECR argon ion production, shown in Fig. 22. Similar results have been reported in other sources /15,16/. The mass dependence of gas mixing can be explained, if energy transfer from the heavy species to the light species is proposed as the mechanism, as illustrated in Fig. 23. Such a cooling process would have an important effect on the ion confinement times, since we have just seen that the energy spread increases at least as fast as  $6.5Q$  eV for highly charged argon ions (see Fig. 21). In this elastic limit, argon would be the best cooling species for argon, but of course no energy can be transferred out of the argon system with argon as the mixing gas.

The possibility that gas mixing is an ion cooling process can also be explored theoretically. The ion confinement times in the Jongen's BALANC code /17/ are determined by ion-ion collision rates. (These calculations generally are very sensitive to the ion temperature.) A later version of this code was modified to allow plasma properties to be input parameters, and this version can be used to 'fit' measured charge state distributions to sets of estimated source parameters /18,19/. We can make a set of plasma parameters fit to the argon-only spectrum in Fig. 22 match the gas mixing spectra of the same figure by changing only the ion energy in the calculation, as shown in Fig. 24.

As a preliminary confirmation of this model, we have measured the energy spread of  $Ar^{9+}$  ions, with and without oxygen gas mixing, and find that energy spread is reduced approximately 25% by the addition of oxygen to the plasma. These measurements are shown in Figs. 25 and 26. If further measurements corroborate this model, there are several immediate consequences. This model suggests that the ion confinement time is limited by the growth of ion energy in sources in where gas mixing has a strong effect. It further suggests that sources that report little or no gas mixing effect probably have very good confinement times as a result other source conditions. There must also be a roll-over effect. While the effectiveness of the mixing species as a coolant increases with mass, so does  $Z$ , so for  $M_2 \approx M_1$ , the average energy of the highly charged ions of these two species would be similar and little or no gas mixing effect would be observed. We do not find neon to be better than

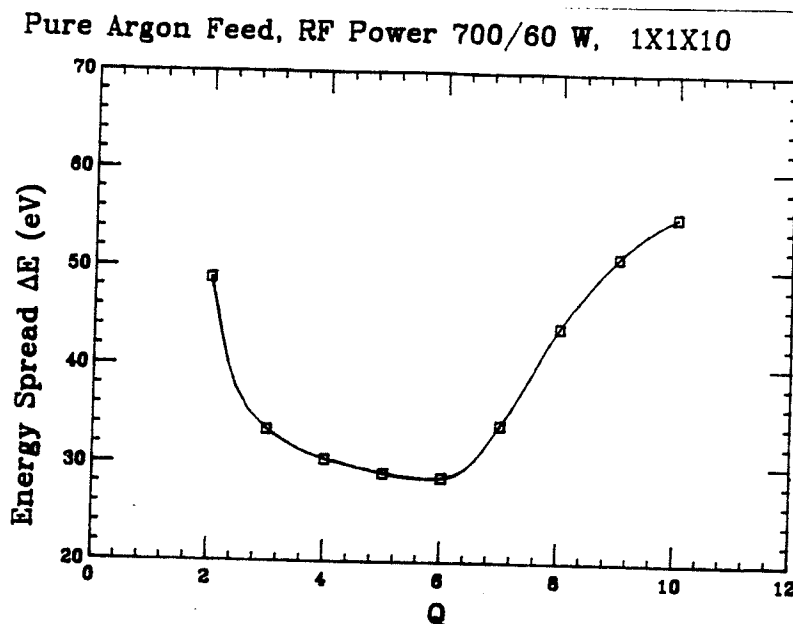


Fig. 21. The dependence of energy spread on the charge of argon ions extracted from the RT-ECR, is shown, tuned for high charge ions with no gas mixing.

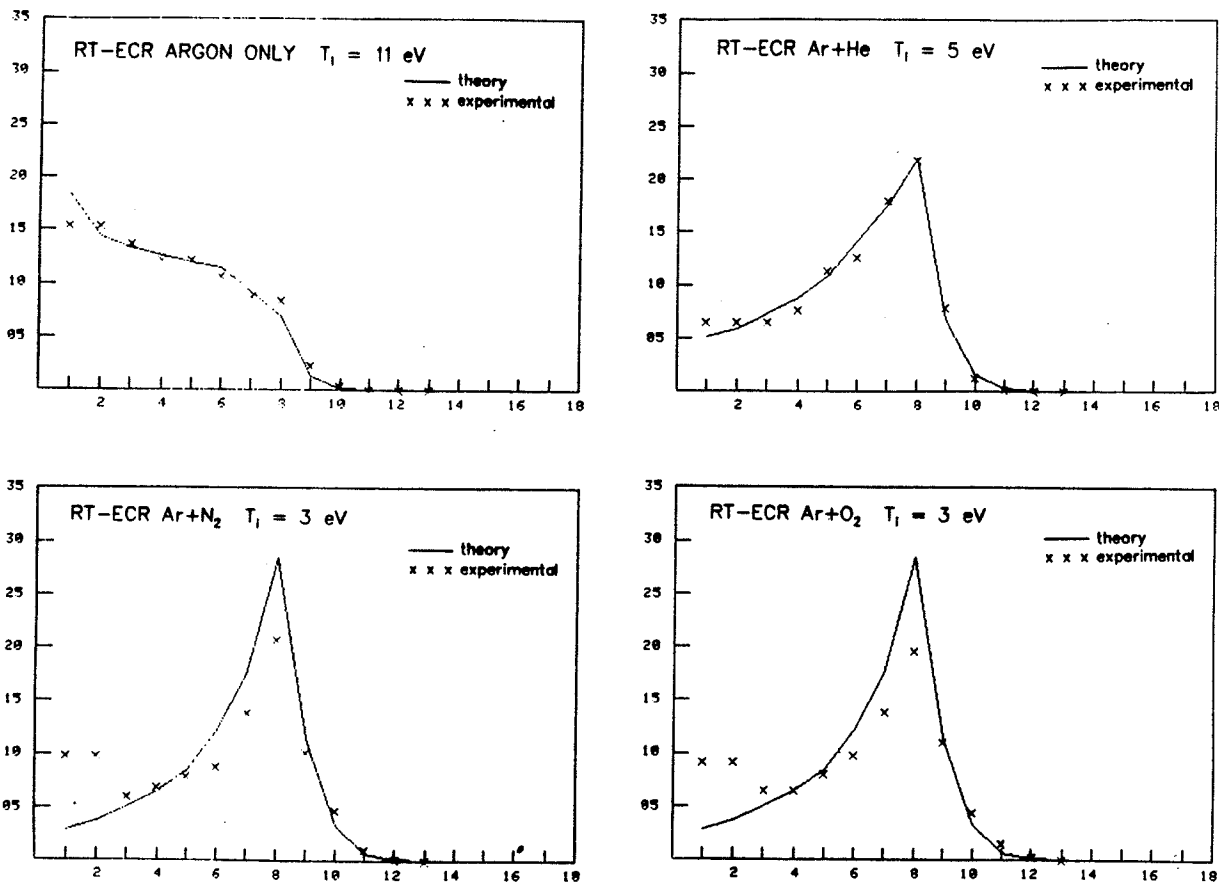


Fig. 24. In the ECRCSD code, ion confinement times are set by ion-ion collisions, subject to the constraint that the plasma losses are balanced. Here we adjust the plasma parameters to fit the argon-only CSD of Fig. 23, and then change only the ion energy. In each case, the gas mixing data of Fig. 23 is fit by decreasing the ion temperature. The code predicts that the temperature is lowered more by gas mixing with nitrogen or oxygen than with helium.

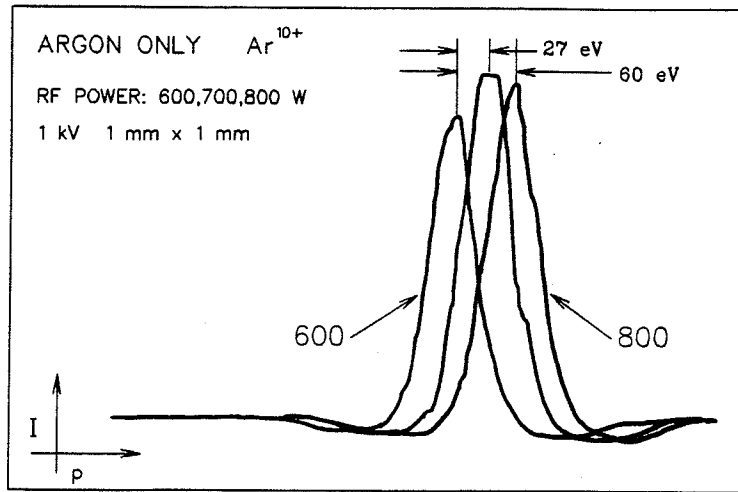


Fig. 27. In this energy spread technique, a shift of a peak to the right indicates an increase in the absolute energy of the ion. We observe that the energy of argon  $10^+$  ions increases as the microwave power injected into the plasma increases.

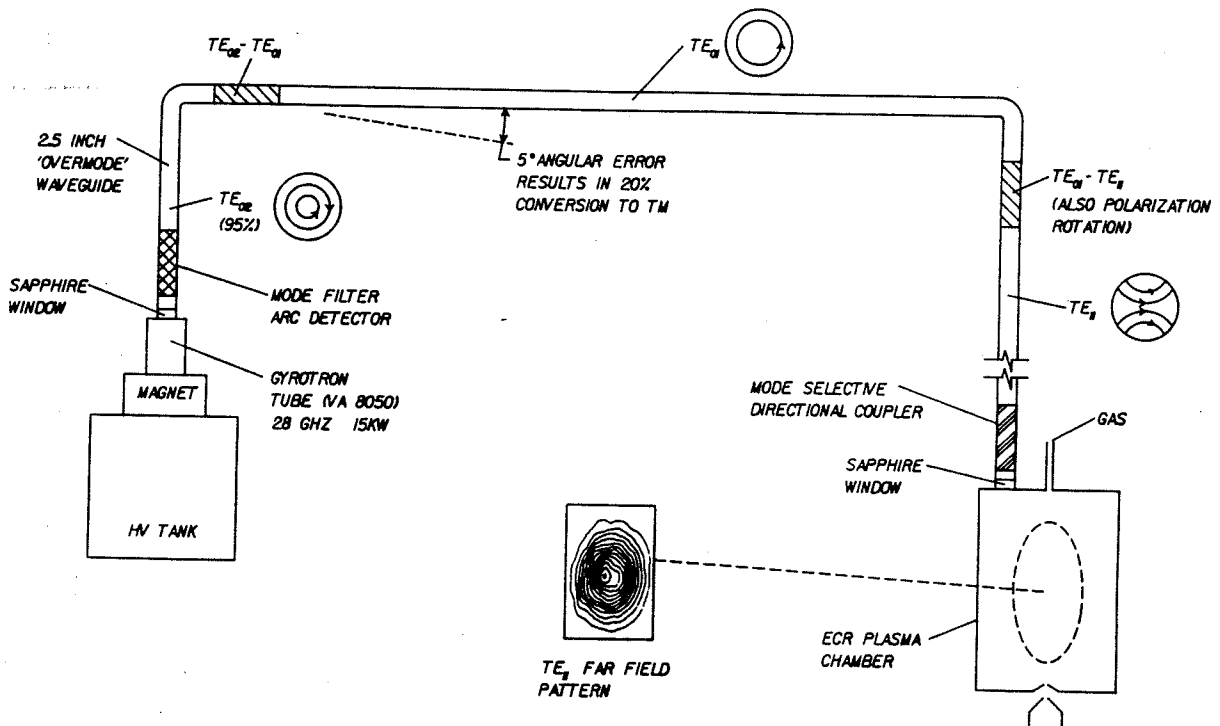


Fig. 28. The initial plan for 28 GHz microwave injection into the SC-ECR from a gyrotron power source emphasizes a maximum of mode control. While probably not essential, power measurement in the waveguide near the source would be improved and the last mode converter can also be used to vary the polarization on the wave to the plasma. The  $TE_{11}$  wave far field pattern, taken from /21/, would peak on axis in the source plasma chamber.

